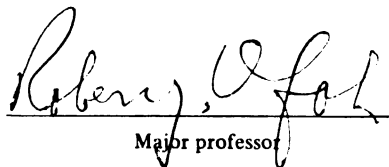This is to certify that the

thesis entitled

A study of the diffusion of bovine serum albumin
at the oil-water interface using total internal
reflection fluorescence and fluorescence photobleaching
recovery

presented by

Parijat Jauhari

has been accepted towards fulfillment
of the requirements for

_____M.S._____ degree in __Chemical Engineering__

Major professor

Date _Aug 18, 1997_

PLACE IN RETURN BOX to remove this checkout from your record.
TO AVOID FINES return on or before date due.
MAY BE RECALLED with earlier due date if requested.

DATE DUE	DATE DUE	DATE DUE

A STUDY OF THE DIFFUSION OF BOVINE SERUM ALBUMIN AT THE OIL-WATER INTERFACE USING TOTAL INTERNAL REFLECTION FLUORESCENCE AND FLUORESCENCE PHOTOBLEACHING RECOVERY

By

Parijat Jauhari

A THESIS

Submitted to
Michigan State University
in partial fulfillment of the requirements
for the degree of

MASTER OF SCIENCE

Department of Chemical Engineering

1997

ABSTRACT

A STUDY OF THE DIFFUSION OF BOVINE SERUM ALBUMIN AT THE OIL-WATER INTERFACE USING TOTAL INTERNAL REFLECTION FLUORESCENCE AND FLUORESCENCE PHOTOBLEACHING RECOVERY

By

Parijat Jauhari

We have combined total internal reflection fluorescence (TIRF) with fluorescence recovery after spot photobleaching (FPR) and fluorescence recovery after pattern photobleaching (FRAPP) to study the diffusion of bovine serum albumin (BSA) labeled with fluorescein-isothiocyanate (FITC) at the oil-water interface. The primary objective was to adapt the TIRF setup used in studies of protein adsorption at the solid liquid interface to make it suitable for the liquid-liquid interface.

We assessed the integrity of our setup by measuring the equilibrium adsorption and diffusion of BSA at the oil-water interface. Diffusion coefficients were obtained by fitting the fluorescence emission data to the diffusion equation, using non-linear regression. We obtained a lateral diffusion coefficient of 3.4×10^{-9} cm^2/s, with a mobile fraction of 0.48; and an apparent bulk diffusion coefficient of 5.2×10^{-8} cm^2/s, with a mobile fraction of 0.77. The difference of one order of magnitude in the two results indicates that bulk diffusion of FITC-BSA is much faster than lateral diffusion, as would be expected. Signal noise and errors in measuring the photobleaching spot size strongly affected the values of the diffusion coefficients.

Dedicated to my parents, to India my country, and to my friends.

Acknowledgments

Table of Contents

Table of Figures

Table of Tables

1. INTRODUCTION

1.1 Motivation for studying the liquid-liquid interface

The liquid-liquid interface is fundamentally important in many biological systems. For example:

1. Liquid-liquid interfaces may have played a role in the origin of life. It has been suggested that the first living cells probably utilized lipid-like hydrocarbon derivatives for their membrane structures. The chemical and physical properties of these oil/water-like interfaces could have contributed to the mechanisms by which energy captured from the environment was used to control photochemical reactions (Deamer and Volkov 1996);

2. the behavior of drugs at biological membranes is an important factor in determining pharmacological activity. Immiscible oil-water interfaces could serve as an artificial model of biomembranes and can, therefore, be used in drug delivery experiments (Arai *et al.* 1996); and

3. the distribution and dynamics of proteins at the liquid-liquid interface is pertinent to many technological processes. In particular, protein adsorption at the liquid-liquid interface is an important component of many processes in the food and pharmaceutical processing industries where proteins are extensively used as stabilizers in emulsions and microemulsions. Information on amphiphilic behavior at the oil-water interface could be used to model these systems. Secondly, studies of protein adsorption at the liquid-liquid interface allow us to gain a better understanding of amphiphile dynamics at this important interface, making it possible to develop better processing and characterization techniques.

1

Various techniques have been used for studying amphiphiles at interfaces. These include scintillation counting, used by Graham *et al.* (1975) to obtain the concentration of proteins at the oil-water interface; monitoring of changes in interfacial tension by Davies and Mayers (1960); Raman scattering, used by Takenaka and Nakanaga (1976), Nakanaga and Takenaka (1977) and Takenaka (1978) to infer the orientation of molecules after adsorption of dyes at the chloroform-water interface; and total internal reflection fluorescence spectroscopy, used by Hirschfield (1965) to examine the fluorescence of dye molecules near an interface.

We have adopted total internal reflection fluorescence (TIRF) as the primary tool in this study, because it is the most suitable for molecular-level investigations of amphiphiles at interfaces. TIRF allows one to excite fluorescent molecules in close proximity to the interface, in preference to those in the bulk. One can then measure the concentration of the fluorophore as a function of distance from the interface, and study the adsorption equilibria and diffusion kinetics of species at the interface. However, most of the published research so far utilizing TIRF has used the technique to study the adsorption and interaction of protein molecules at the solid-liquid interface. Our goal was to modify the standard TIRF technique to make it suitable for application at the liquid-liquid interface.

1.2 Objectives of this study

The specific objectives of this project were to:

1. modify the total internal reflection fluorescence technique used for the solid-liquid interface to make it suitable for application at the liquid-liquid interface, and to incorporate capabilities for fluorescence photobleaching recovery (TIRF/FPR) and fluorescence recovery after pattern photobleaching (TIRF/FRAPP);

2. establish qualitatively the relative importance of bulk and surface diffusion of a representative protein at the liquid-liquid interface, using both pattern photobleaching and spot photobleaching; and

3. determine the lateral and bulk diffusion coefficients of bovine serum albumin (BSA) at the oil-water interface, using both spot (FPR) and pattern photobleaching (FRAPP).

2. THEORETICAL CONSIDERATIONS

Total internal reflection fluorescence (TIRF) was first used by Tweet *et al.* (1964) to measure the emission spectrum and quenching behavior of *chlorophyll a* monolayers at the air-water interface. TIRF was used to exclude the signal from direct and scattered mercury arc excitation, so only the weak fluorescence generated by the dilute monolayer would be detectable. TIRF has also been used at the oil-water interface by Morrison and Weber (1987) to study the adsorption of 4,4-bis-1-phenylamino-8-napthalenesulfonate (bis-ANS) at the decalin-water interface.

The theory of total internal reflection fluorescence has been described in detail in many references, such as Axelrod *et al.* (1981), Axelrod (1990), and Axelrod *et al.* (1992). The theory of spot photobleaching has been described by Axelrod *et al.* (1976), Barisas and Leuther (1979), Elson (1985), Lanni and Ware (1984), and Webb and Thomas (1990). Fluorescence recovery after pattern photobleaching has been described by Abney *et al.* (1992), Robeson (1995), Robeson and Tilton (1995), and Tilton *et al.* (1990 a, b). Therefore, only the details relevant to this study would be presented here.

2.1 Total internal reflection

When a beam of light is incident upon an interface made up of materials of different refractive indices at an angle θ greater than a given critical angle, it is totally internally reflected in the optically denser medium (refractive index of n_1). The critical angle, θ_c, is given by

$$\theta_c = \sin^{-1}\left(\frac{n_2}{n_1}\right) \qquad (n_1 > n_2) \qquad [1]$$

As a result of this total internal reflection, an evanescent field is formed in the optically

4

As a result of this total internal reflection, an evanescent field is formed in the optically rarer medium with an exponentially decaying intensity, as shown in Figure 1. The intensity of the evanescent wave is given by

$$I = I_0 \exp\left(-\frac{z}{d}\right)$$ [2]

where I is the scattering intensity at z, I_0 is the scattering intensity at the interface and d is the depth of penetration of the evanescent wave, which is given by

$$d = \frac{\lambda_0}{4\pi n_1 \sqrt{\sin^2 \theta - n_{21}^2}}$$ [3]

Here, λ_0 is the wavelength of the incident radiation in vacuum and n_{21} is the relative refractive indices of the two media:

$$n_{21} = \frac{n_2}{n_1}$$ [4]

The exponentially decaying evanescent field is a powerful tool to selectively excite species in the vicinity of an interface, and to study their interactions.

2.2 Fluorescence Recovery After Photobleaching

In this technique, a brief pulse of strong laser light is flashed at the interface, photobleaching all of the fluorescent species in the field of the beam. The subsequent recovery of the signal towards the prebleach level by exchange of bleached non-fluorescent species with unbleached fluorescent species is observed using a monitoring beam (a laser beam of much less intensity).

The photobleaching recovery characterizes the rate at which the unbleached molecules diffuse, hence it gives a measure of the transport characteristics of the species. In this study, two modes of photobleaching (spot photobleaching and pattern photobleaching)
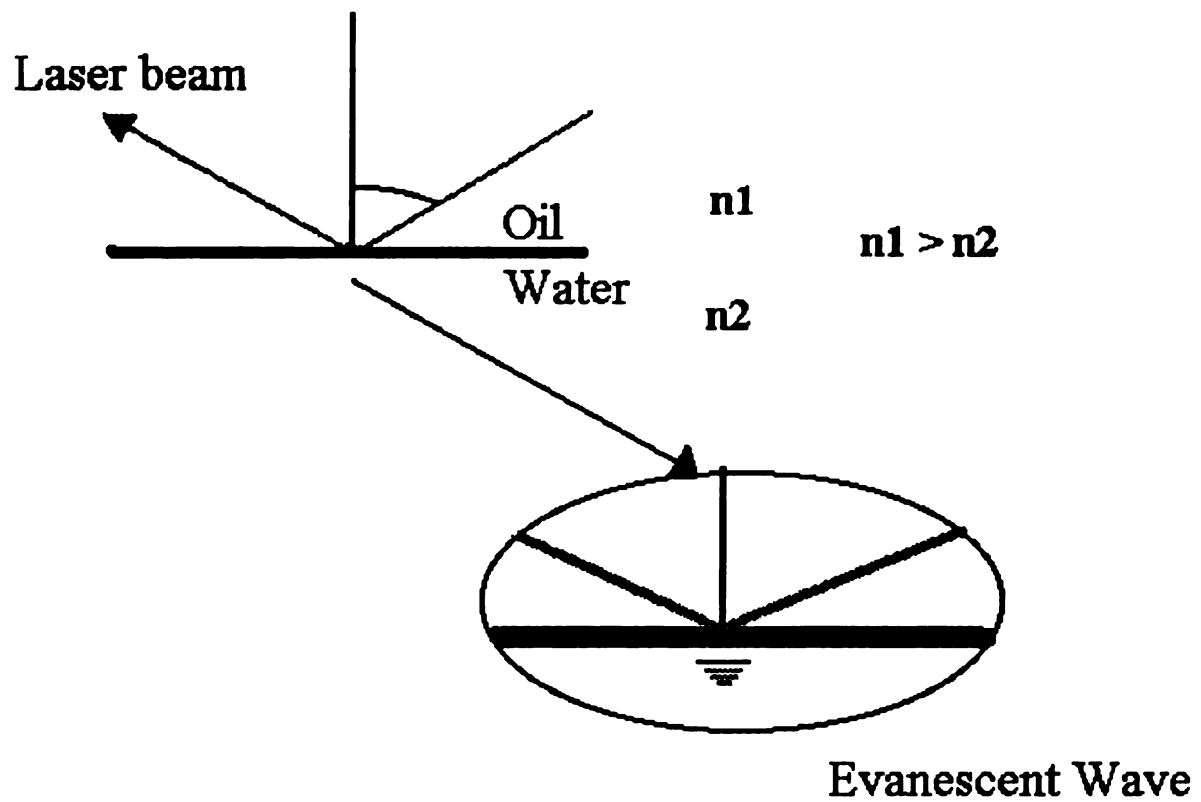
Figure 1. Total internal reflection induced by a laser beam incident on an interface made up of materials of different refractive indices.

were used to obtain information about the lateral and bulk diffusion coefficients of BSA proteins tagged with the FITC fluorophore.

2.2.1 Spot Photobleaching

In spot photobleaching, a small spot is bleached at the interface. The photobleached spot has a characteristic length l and a recovery time constant of τ. These two variables are related to the diffusion coefficient D by

$$\tau = \frac{l^2}{D} \qquad\qquad [5]$$

Thus, if we vary the length of the spot and measure the recovery time, then we can use the plot of τ versus l^2 to obtain the surface diffusion coefficient, $D_{surface}$. Conversely, if we vary the penetration depth of the evanescent wave d, while keeping l constant, then a plot of τ versus d^2 would enable us go get the bulk diffusion coefficient, D_{bulk}. This procedure gives both qualitative and quantitative information about the relative importance of the two modes of diffusion.

2.2.2 Pattern Photobleaching

In pattern photobleaching, two beams of equal intensity are intersected and totally internally reflected at the interface. The interference pattern formed by the evanescent waves from the two beams is used to photobleach molecules adsorbed at the interface. The experimental setup for pattern photobleaching is more complicated than the one for spot photobleaching. However, it has two advantages over spot photobleaching. It allows one to more accurately control the characteristic length of the illuminated region by varying the angle of incidence. It also allows the measurement of smaller length dimensions, compared to spot photobleaching (Abney et al. 1992).

3. EXPERIMENTAL MATERIALS AND TECHNIQUES

3.1 Experimental equipment

3.1.1 Setup for TIRF experiments

The TIRF setup consists of a 5-W Lexel 95 continuous wave argon ion laser (Lexel Lasers, Inc., Fremont, CA), an inverted microscope (Axiovert 135 M, Carl Zeiss Inc., Thornwood, NY) and a photomultiplier tube (PMT) system using a modular automation controller (MAC 2000, Ludl Electronic Products Ltd., Hawthorne, NY) with a Hamamatsu R928 standard tube. Using an arrangement of flats and mirrors, as shown in Figure 2, the laser beam was split into a monitoring beam and a photobleaching beam and directed at the interface where the fluorescence emission was collected by a PMT.

The 5-W argon ion laser allowed us to photobleach and monitor the interface with the same light source. Using a microscope allowed us to incorporate capabilities for bright-field, dark-field, phase contrast and epi-illumination techniques into the setup, if needed. Using one flat to split the laser beam into a monitoring and photobleaching beam and then recombining the beams using another flat ensures a perfect alignment of the monitoring beam and the photobleaching beam (Thomas and Webb 1990).

A shutter (D122, Vincent Associates, Rochester, NY) allowed us to control which light beam would reach the interface. When the shutter was closed, only the monitoring beam was directed to the interface; when it was open, both the photobleaching and monitoring beams are focused on the interface. To make this possible, we cut a hole in the shutter to enable the monitoring beam to be always incident on the interface while making measurements. To increase the signal to noise ratio, the PMT was jacketed inside a water-cooled housing system (TE177TSRF, Products for Research, Inc., Danvers, MA) which maintained a constant temperature around the tube and reduced the noise level.
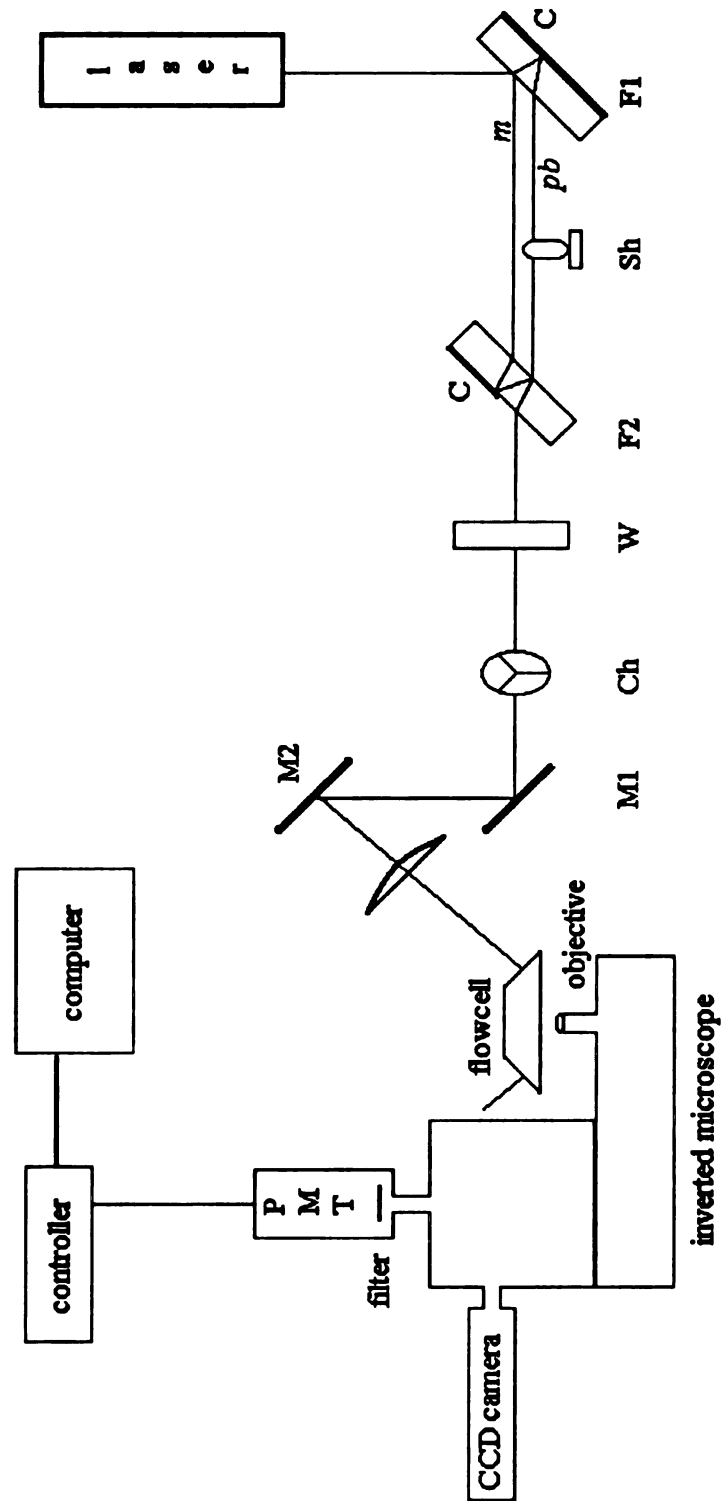
9

Figure 2. Setup for total internal reflection fluorescence experiments, showing the optical components used to direct the beam to the oil/water interface.

We used a computerized data acquisition system with the Viewdac software (Keithley Instruments, Inc., Rochester, NY) for data collection. This allowed us to gather a large quantity of data over short periods of time. A CCD camera (MTI, VE 1000, Carl Zeiss Inc., Thornwood, NY) was used to focus the laser beam into the experimental cell without having to look through the eyepiece. We also have the capability to take pictures of the interface using a 35-mm camera (Contax 167MT, Yashica Inc., Somerset, NJ).

The whole setup was housed on a vibration isolation table (RS 4000, Newport Corporation, Irvine, CA). The table floats on a cushion of air and prevents building vibrations from destabilizing the oil-water interface.

3.1.2 FRAPP Setup

The setup shown in

Figure 3 was adapted from the apparatus used by Robeson (1995) to measure surface diffusion of bovine serum albumin on polymeric substrates. The laser beam was split into two beams of equal intensity, using a 1-inch cubic non-polarizing beamsplitter (Newport Corporation, Irvine, CA). The two beams were then directed to meet at the interface using an arrangement of two mirrors, a cubic beamsplitter and a focusing lens. One of the mirrors was mounted on a miniature piezo-flexure mirror mount (17 ASM 001,Melles Griot, Inc., Boulder, CO) and was driven by a piezo electric controller (17 PCS 001, Melles Griot). This arrangement allowed fine focusing of the two beams so they would intercept at the interface. It was also used to calculate the amplitude of the interfering beam pattern as described later in Chapter 4.

3.1.3 The experimental cell

The experimental cell shown in Figure 4a forms the heart of the setup. It consists of a top microscope slide (Fisher Scientific, Pittsburgh, PA) optically coupled with an immersion oil (16482, type A, R.P. Cargille Laboratories, Inc., Cedar Grove, NJ) to a dovetail prism
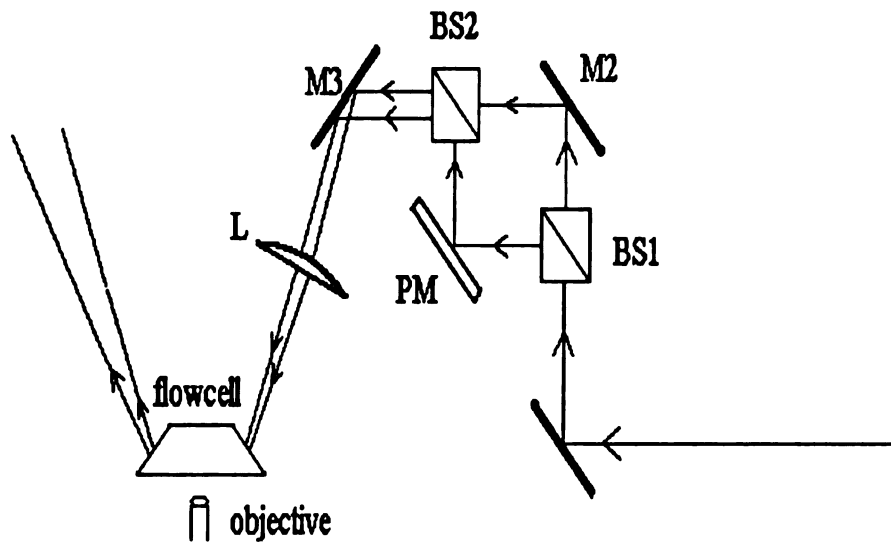
BS1, BS2 - Beamsplitters , M1, M2,M3 - Mirrors, L - Focussing lens, PM - mirror mounted on the nanoflex mount and connected to the piezo electric driver

Figure 3. Optical configuration used for FRAPP experiments (after Robeson 1995). The setup produces two intersecting beams at the interface to create the fringes required for pattern photobleaching.

expanded view of the oil-water interface

THE FLOWCELL

a. front view

Prism

Incident Laser Light

proteins

$\theta > \theta_c$

Top Glass Slide

Aluminium Spacer

Protein solution in contact with oil

O-rings

Bottom Glass Slide

Teflon Tubing

To Syringe Pump

b. top view

O-ring
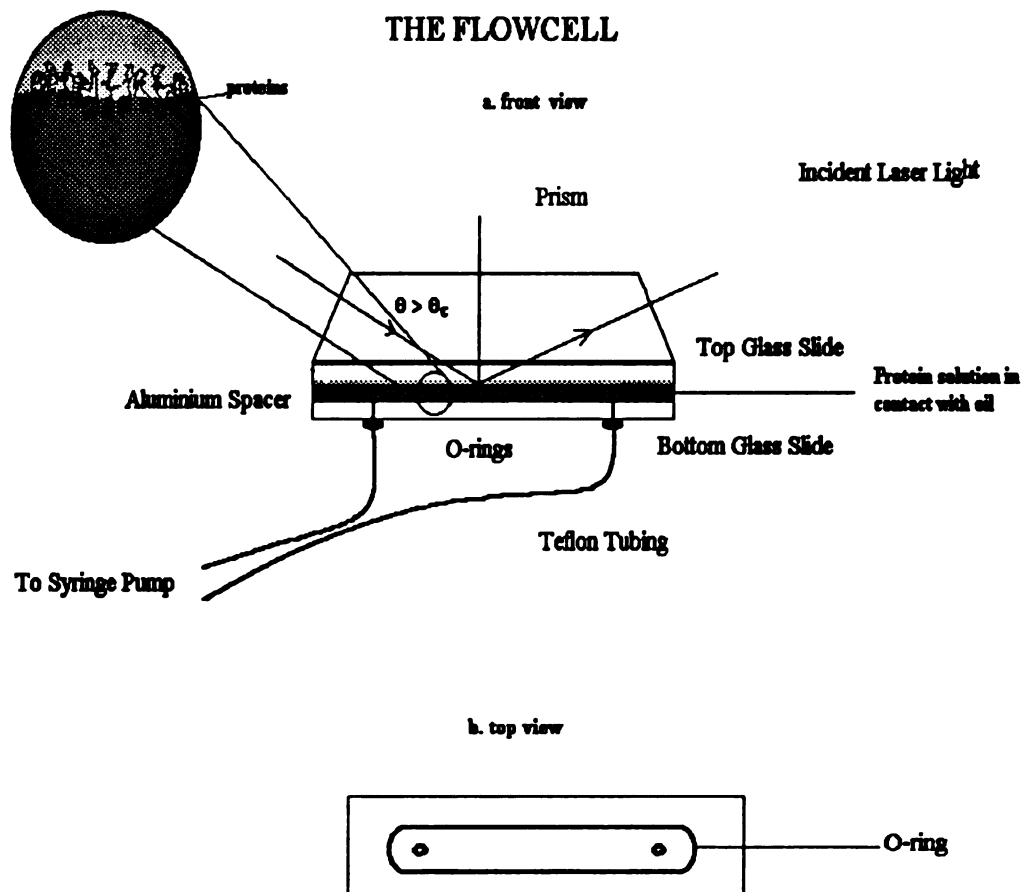
Figure 4. Components of the experimental cell. While all experiments were conducted under stopped-flow conditions, the cell can also be used as a standard flow cell.

of angle 64⁰. The bottom of the top slide is coated with the same immersion oil and serves as the oil part of the interface (the complete formation of the oil-water interface is given in the next section). Below the top slide, we have an aluminum spacer of the same dimension as the slide, and a bottom slide to complete the cell assembly.

The spacer has a channel cut into it (Figure 4b). When the channel is filled with water or protein solution and the top microscope slide is placed over the cell, an oil-water interface is formed with the oil coating on the bottom of the top slide. An O-ring (Parker Seals, NJ) is inserted into the spacer channel, and used to seal the cell to prevent leakage of the protein solution. The bottom slide has two holes drilled into it (Figure 4b) which allow us to connect a syringe pump to the experimental cell for infusing and withdrawing the protein solution. The whole assembly of the prism, top slide, aluminum spacer and the bottom slide is tightly screwed on to an anodized aluminum shell, and sits on the top of the microscope stage during experiments.

While all experiments were conducted under stopped-flow conditions, the experimental cell can also be used as a standard flow cell.

3.2 Material preparation procedures

3.2.1 Protein labeling

For the purpose of studying interactions at the oil-water interface, bovine serum albumin (BSA) (A-7511, Sigma Chemical Co., St. Louis, MO) was labeled with Fluorescein-5-isothiocyanate (F-1907, Molecular Probes, Eugene, Oregon). Also albumin, bovine-fluorescein isothiocyanate (A-9771, Sigma Chemical Co., St. Louis, MO) with a labeling ratio of approximately 12:1 was mixed with unlabelled BSA to obtain the appropriate labeling ratios needed to avoid concentration quenching of the signal. A buffer of concentration 0.1 M and pH of 9 was made from Borax (B-9876, Sigma Chemical Co.), and was used as in all the labeling reactions and for making all the protein solutions.

Protein concentrations were kept below the critical micelle concentration (cmc); therefore, only single particle interactions have been characterized in this study. The procedure used to label the proteins and calculate their labeling ratios has been described by McKinney *et al.* (1965).

3.2.2 Coating of bottom slide in experimental cell

A 0.5 wt% solution of polyethylene oxide (PEO) with a molecular weight of $8x10^6$ (37,283-8, Aldrich Chemical Company, Inc., Milwaukee, WI) was made with deionized water. A clean microscope slide was soaked in the PEO solution for 2 hours, causing a film to be formed on the quartz slide. The slide was then washed with water to remove any excess PEO. The film coating on the bottom slide of the sample cell was applied to prevent the adsorption of proteins at the bottom interface formed by the glass and water (Cheng *et al.* 1987).

3.2.3 Immobilization of fluorophore

A 15 wt % solution of Gelatin (Knox, Nabisco Inc., Hanover, NJ) was made in warm Borax buffer (0.1 M, pH ~ 9). Approximately $1.5x10^{-3}$ M FITC was reacted with the boiling gelatin solution for about one hour. The moist solution was then spin-cast onto a clean slide. The slide, with the immobilized fluorophores, was used in experiments to calculate the amplitude of the fringes and the bleaching parameter k (Robeson, 1995), as described later. The slide was also used in the calibration process to calculate the instrument constant of the TIRF setup.

3.3 Experimental Techniques

3.3.1 Formation of the Oil-water interface

The oil-water interface was formed with an immersion oil (16482, type A, R.P. Cargille Laboratories, Inc., Cedar Grove, NJ) in contact with distilled deionized water. The following procedure was used in preparing the interface:

1. Each slide was cleaned using the procedure described by Cheng *et al.* (1987), and heated for 15 minutes under a heat lamp.

2. A drop of oil was placed in the center of the slide, where it quickly spread over the slide to form a thin film of oil.

3. The slide was then optically coupled to a prism with the same immersion oil used to form the oil-water interface.

4. The slide and the prism were then placed on top of the sample cell filled with buffer or protein solution to form the oil-water interface. We estimated the oil layer in contact with the water to be approximately 100 μm thick.

3.3.2 Introduction of proteins into the experimental cell

The sample cell was first filled with a buffer solution to establish the oil-water interface. Then the protein solution was pumped into the cell using a double syringe pump which withdrew the buffer solution from the cell at the same rate as the protein solution was pumped. The solution was allowed to flow into the cell until the buffer solution in the cell has been completely displaced by protein solution. At that time, the syringe pump was turned off, and a stable interface re-established. Our goal was to put the oil layer into contact with a protein solution approximately 1 mm thick, which is thin enough to allow us to simultaneously accomplish two objectives: 1) give an equilibrium adsorption time on the order of minutes rather than hours; and 2) provide the ability to use hydrodynamic shear to sweep the interface clean within a reasonable amount of time.

3.3.3 FPR experimental protocol

The FPR experiments were conducted according to the procedure described by Axelrod *et. al* (1976). The protein solution was introduced into the sample cell and adsorption was allowed to proceed to steady state, as determined by a constant fluorescence signal. We then photobleached a spot at the interface and measured the rate of fluorescence recovery.

3.3.4 FRAPP experimental protocol

All FRAPP experiments were conducted with 0.067mM FITC-BSA (labeling ratio of 1.06) adsorbed at equilibrium at the interface, with unlabelled BSA of the same concentration in the bulk. First we passed Borax buffer through the cell. We then introduced FITC-BSA at the same flow rate into the sample cell. After steady state had been reached, we introduced unlabelled BSA at the same flow rate into the cell and allowed the system to reach steady state, again as indicated by a constant fluorescence signal (Tilton *et. al* 1990). After steady state had been reached, we photobleached the interface and observed the rate of fluorescence recovery.

The introduction of unlabeled BSA into the sample cell serves two purposes. It allows the exchange of loosely bound FITC-BSA with unlabelled BSA, so only the mobility of irreversibly surface bound proteins is measured. It also assures us that any signal obtained is from the irreversibly bound proteins at the interface and not from the bulk. Since we allowed the system to reach steady state after introducing unlabeled BSA, any drop in fluorescence measured during photobleaching will only be due to the lateral exchange of surface bound species. Essentially, we have assumed that any exchanges between unlabeled BSA and FITC-BSA would have also reached a steady state.

The same experimental cell was used for all FRAPP experiments, simply by choosing different spots, at the interface. Since the time constant for the exchange of species at the interface by lateral diffusion is much larger than the time scale of our experiments, this approach should not present a problem by introducing experimental artifacts.

3.3.5 Experimental precautions

The following precautions were observed during all FRAPP experiments:

1. The mirrors and optics were kept clean and fixed so that the Gaussian profile of the laser beam is not disturbed and the fringe pattern does not shift during measurements.

2. The microscope was focused exactly at the interface so that the focal plane and the plane where the fringes are formed are the same.

There was always a concern about unintended photobleaching of adsorbates by the monitoring beam, particularly when adsorption is very slow to reach equilibrium and the monitoring beam is left on for an extended period of time (Axelrod 1990). A beam chopper was used during long adsorption experiments to reduce the total amount of radiation reaching the interface, and to prevent unintended photobleaching of the fluorophores.

Flow cells such as our sample cell are routinely used in studies at the solid-liquid interface without the risk of destroying the interface, even during flow. With the liquid-liquid interface, however, there is a strong possibility of sweeping away adsorbed molecules as a result of shear imposed on the interface by the flowing fluid. A double syringe pump which simultaneously infuses and withdraws very minute quantities of liquid was used to prevent shear from clearing the interface. As a further precaution, nearly all the experiments were conducted in stopped-flow situations.

To obtain the maximum allowable flow rate to be used for pumping protein solutions during flow situations, we conducted a number of replicate experiments in which we:

1. Introduced the protein solution into the sample cell and measured the fluorescence
2. Then we introduced a buffer solution and measured the fluorescence emission again.
3. We then reintroduced the same concentration of protein solution used in step 1, and measured the fluorescence emission again.

At a flow rate of 0.17 ml/min, the fluorescence emissions from introduction of protein in steps 1 and 3 were statistically the same (fluorescence versus time, in arbitrary but consistent units) as shown in Figure 5. Also no oil was found either in the syringe or the tubing connected to the experimental cell. This assured us that we were not destroying the oil-water interface during periods of flow.
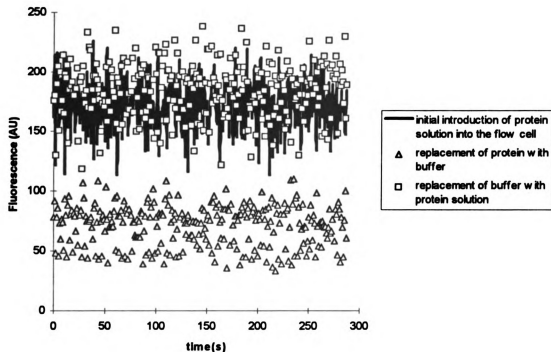
Figure 5. Protein adsorption experiment conducted to assess the effect of flow rate on the integrity of the oil-water interface. Fluorescence emissions from identical protein solutions (introduced before and after the cell was filled with a buffer) were statistically the same at flow rates of 0.17 ml/min and lower.

3.4 Determination of interfacial concentrations of fluorophores on the basis of fluorescence emission data

Devising a reliable calibration technique for the quantification of the surface concentration of amphiphiles based on a given fluorescence signal is a difficult problem at the liquid-liquid interface, in comparison to the solid-liquid interface. A number of approaches have been used to determine the interfacial concentrations at the solid-liquid interface which are made possible by the fact that a) protein adsorption is irreversible at this interface, and b) the interface is non-mobile and stable. These techniques include depletion of adsorbates in the bulk phase (Burghardt and Axelrod 1981), use of non-adsorbing species (such as polystyrene spheres) as a standard, use of scintillation counting coupled with TIRF (Lok *et al.* 1983a,b) and combination of reflectometry with TIRF (Robeson 1995).

Unfortunately, none of these techniques will work at the liquid-liquid interface, due to two limitations:

1. There is no reliable technique that can be used to drain the bulk solution from the sample cell without incorporating adsorbed species as well as the oil layer in the effluent, even if we assume that adsorption is irreversible at this interface.

2. Quantitation methods such as combining reflectometry or scintillation counting with TIRF rely on the immobilization of proteins due to irreversibility of adsorption at the solid-liquid interface. As a result, the solid can be removed from the sample cell and the quantity of adsorbed species determined accurately by any one of several methods. This approach is not feasible at the liquid-liquid interface.

To circumvent these difficulties, we propose a calibration technique here that uses the experimental cell along with photobleaching recovery to determine the interfacial concentration of adsorbed species *in situ*, without destabilizing the oil-water interface. The theoretical basis for this technique is presented below.

The intensity of fluorescence emission, F, from proteins at the interface and in the bulk is given by

$$F = \int_0^\infty I(z)C(z)g(z)dz \qquad [6]$$

where $I(z)$ is the intensity of the incident beam and varies with depth, $C(z)$ is the concentration of the fluorescent species, and $g(z)$ is a function which depends on the relative quantum yield of the fluorescent species and on instrument characteristics. The integral quantum yield of molecules adsorbed at the interface and those in the bulk can be different. However, Zimmerman *et al.*(1990) and Robeson (1995) have shown that the quantum yields of proteins adsorbed at the solid-liquid interface and in the bulk do not differ appreciably. Also, at labeling ratios below the concentration at which quenching occurs (as is the situation in this case), the relative quantum yield is constant. Therefore we can rewrite equation [6] as

$$F = g\int_0^\infty I(z)C(z)dz \qquad [7]$$

Substituting equation [2] into [6] we get

$$F = I_o g\int_0^\infty e^{-z/d}C(z)dz \qquad [8]$$

For immobilized fluorophores, we can make the following substitutions:

1. The evanescent wave extends to Δ, the thickness of the immobilized fluorophore film. Therefore, we can change the upper limit of the above integral to this variable.

2. Because of the uniformity of the matrix, $C(z)$, the concentration of the immobilized fluorophores (BSA-FITC immobilized in gelatin) is uniform and can be set equal to C at both the interface and in the bulk.

Incorporating these, we can rewrite equation [8] as

$$F = KC\int_0^\Delta e^{-\frac{z}{d}} C\,dz = KC\left[-de^{-\frac{z}{d}}\right]_0^\Delta = KC\left(-de^{-\frac{\Delta}{d}}+d\right) \qquad [9]$$

where K is a proportionality constant which incorporates the relative quantum yield and the intensity of the incident laser beam. K is referred to as the instrument constant, and is unique to each setup.

Since $\Delta >> d$, equation [9] reduces to

$$F = KdC \qquad [10]$$

The result is that, since F, d and C are all known, we can evaluate K.

For a protein adsorbing from a bulk solution to the oil-water interface, we can assume that a simple monolayer is formed at the interface in equilibrium with the bulk concentration of proteins (Zimmermann et al. 1990). We can also assume that this layer of adsorbed molecules has a thickness l and a surface concentration C_s (units of mass or moles per area). For a monolayer of proteins at the liquid-liquid interface, the thickness l corresponds approximately to the diameter of the hydrophilic head of the protein, assuming that the hydrophobic segment of the protein penetrates into the oil layer and is, therefore, not observable by the evanescent wave.

Incorporating this, we can rewrite equation [8] as a sum of the fluorescence emission from the interface $(0 \le z \le l)$ and from the bulk solution $(l \le z \le \delta)$:

$$F = K\left(C_s + \int_{l}^{\delta} e^{-\frac{(z-l)}{d}} C_b \, dz\right) \qquad [11]$$

where C_b is the concentration of the fluorescent species in the bulk (units of mass or mole per volume), and δ is the depth of the sample cell.

We know that l is approximately 3nm (Zimmermann et. al 1990). Also, d is 138 nm for our setup, and δ is 1 mm. Therefore,

$$\int_{l}^{\delta} e^{-\frac{(z-l)}{d}} C_b \approx dC_b \qquad [12]$$

Substituting [12] into [11] we get

$$F = K(C_s + dC_b)$$ [13]

If a bleaching pulse is flashed at the interface, the recovery of bulk emission should be almost instantaneous, in comparison to the emission from the surface because of the different transport time scales for bulk and surface diffusion. This means that diffusion in the bulk will lead to a rapid replacement of the bleached protein molecules by unbleached ones, and will be observed as a partial recovery of fluorescence. Since this signal is entirely from the bulk, equation [13] becomes

$$F_{bulk} = KdC_b$$ [14]

Combining equations [13] and [14], we can calculate the interfacial concentration of amphiphiles:

$$C_s = \frac{F - F_{bulk}}{K}$$ [15]

Using Eq. [15], a plot of C_s versus F will yield the surface concentration at any fluorescence intensity.

Three assumptions are implicit in this analysis:

1. exchange of proteins adsorbed at the interface with the bulk species is very slow compared to the time scales of the experiment (for both lateral and bulk diffusion);

2. K, which is the product of the instrument constant and the quantum yield of the species, is constant in the specified concentration range and over the time scales of the experiment; and

3. The glass-gelatin and oil-water interfaces have identical critical angles for total internal reflection. This assumption is supported by Robeson (1995) who reported that, due to its high water content, gelatin has essentially the same refractive index as water.

3.5 Data analysis procedures

The procedure developed by Axelrod *et al.* (1976) was used for analyzing the spot photobleaching data, and the Robeson (1995) procedure was used for FRAPP analysis. The theoretical basis of the two procedures are briefly outlined here.

When two coherent plane polarized beams intersect at an interface, the intensity of the resulting interference pattern varies spatially as

$$I(x) = I_o(1 + A \sin(\pi x / w)) \qquad [16]$$

where w is the fringe width and A is the amplitude of the interfering fringes (Robeson 1995). For spot photo bleaching, the spatial intensity of a Gaussian beam varies as

$$I(r) = \frac{2P}{\pi R^2} \exp\left(-\frac{2r^2}{R^2}\right) \qquad [17]$$

where P is the power of the laser beam and R is the half width of the laser beam at a depth of $1/e^2$ (Axelrod *et al.* 1976).

The diffusion of proteins in the absence of convection is governed by Fick's second law

$$\frac{\partial C}{\partial t} = D \frac{\partial^2 C}{\partial^2 r} \qquad [18]$$

where C is the concentration of the diffusing species, D is the diffusion coefficient, t is the time of diffusion and r is the position vector of the species.

Due to the large aspect ratio of the fringes, only diffusion in a direction perpendicular to the fringes contributes significantly to the fluorescence recovery, so equation [18] can be rewritten in one dimension and in non-dimensional form as (Robeson 1995)

$$\frac{\partial C}{\partial T} = \frac{\partial^2 C}{\partial X^2} \qquad [19]$$

where $X = x/w$ and $T = Dt/w^2$.

We can calculate w from (Axelrod 1990)

$$w = \frac{\lambda_o}{2n_3 \sin\theta \sin(\beta/2)}$$

[20]

where β is the angle formed by the two beams in the plane of TIR. Therefore, by directly measuring θ and β, the fringe width can be calculated. Another more accurate way to calculate the fringe width is to insert a calibrated reticule in the eyepiece of the microscope and measure the fringe width directly.

The concentration profile immediately after photobleaching is given by

$$C(X,0) = \bar{C}e^{-kI(X)}$$

[21]

where $\bar{C}$ is the concentration before photobleaching, and k is the bleaching parameter which contains the rate constant for photobleaching and the duration and intensity of the photobleaching pulse (Axelrod $et\ al.$ 1976).

The fluorescence recovery profile following photobleaching is given by

$$F(t) = \int I(r,\theta)C(r,\theta,t)q_r(C)dA$$

[22]

The task now is to determine the functional form of $C(r,t)$ so that equation [22] can be integrated. This problem has been solved by Robeson (1995) and Axelrod (1976) for pattern and spot photobleaching, respectively.

The solution of the diffusion Dirichlet problem in the domain $(-1 < X < 1)$ and $(0 < t < \infty)$ for FRAPP is given by (Robeson 1995)

$$C(X,T) = \frac{a_0}{2} + \sum_{n=1}^{\infty} \exp(-n^2\pi^2 T)[a_n \cos(n\pi X) + b_n \sin(n\pi X)]$$

[23]

where a_n and b_n are Fourier coefficients given by

$$a_n = \int_{-1}^{1} \exp(-kI(X)) \cos(n\pi X) dX \qquad [24]$$

$$b_n = \int_{-1}^{1} \exp(-kI(X)) \sin(n\pi X) dX \qquad [25]$$

Similarly, for spot photo bleaching, the concentration profile is given by (Axelrod *et al.* 1976)

$$C(r,t) = \bar{C} \sum_{n=0}^{\infty} \frac{(-k)^n}{n!} \left(\frac{R^2}{R^2 + 8nDt} \right) \exp\left[-\frac{2nr^2}{8nDt + R^2} \right] \qquad [26]$$

Equation [23] or [26] can be substituted, as needed, into equation [22] to obtain the fluorescence recovery profiles, assuming constant quantum yield. After carrying out the integration, Robeson (1995) obtained the following equation for the fluorescence recovery profile after pattern photobleaching

$$F(t) = (F_o - \bar{F}) \left[1 - \frac{Ab_1 f}{2 - a_o - Ab_1} \left(1 - \exp\left\{ \frac{t}{\tau} \right\} \right) \right] + \bar{F} \qquad [27]$$

Here, F_o is the prebleach signal, $\bar{F}$ is the signal immediately after photobleaching, f is the mobile fraction of molecules and a_o and b_1 are the Fourier coefficients given by equations [24] and [25], and τ is the characteristic diffusion time for pattern photobleaching:

$$\tau = \frac{w^2}{\pi^2 D} \qquad [28]$$

The same integration process, when carried out for spot photobleaching, gives the following solution (Axelrod *et. al* 1976)

$$F(t) = \bar{F} \sum_{n=0}^{n=\infty} \frac{(-k)^n}{n! \left[1 + n\left(1 + \frac{2t}{\tau} \right) \right]} \qquad [29]$$

where τ is the characteristic diffusion time for spot photobleaching with a Gaussian beam:

$$\tau = \frac{w^2}{4D} \tag{30}$$

For small k values, equation [29] can be simplified to (Axelrod et. al 1976):

$$F(t) = \bar{F}\left(1 - \frac{k}{2\left[1 + \frac{t}{\tau}\right]}\right) \tag{31}$$

The mobile fraction f is given by

$$f = \frac{F_0 - F(\infty)}{F_0 - \bar{F}} \tag{32}$$

where $F(\infty)$ is the asymptote of the fluorescence recovery curve.

Similarly if the amplitude of the interfering fringes is close to unity, we can rewrite equation [27] as

$$\frac{F(t) - \bar{F}}{F_0 - \bar{F}} = 1 - \frac{f}{3} + \frac{f}{3}e^{-\frac{t}{\tau}} \tag{33}$$

and f can be calculated either by non linear regression of this equation or by (Tilton et. al 1990a)

$$f = 3\left(\frac{F_0 - F(\infty)}{F_0 - \bar{F}}\right) \tag{34}$$

Experimental data were fit to equations [31], [32], [33] and [34] to obtain the diffusion coefficients and the mobile fraction of FITC-tagged BSA proteins at the oil-water interface.

3.6 Calculation of the amplitude of the fringe pattern

Ideally, the spatial amplitude of the fringe pattern should be unity. However, if the two intersecting beams are not perfectly at critical angle, the amplitude will be less than unity. We used the process described by (Robeson 1995) to calculate the amplitude of the interfering fringe pattern created by the intersecting beams.

We bleached the surface of the slide containing the immobilized fluorophores, and observed the fluorescence recovery using the monitoring beam. When the monitoring beam pattern was shifted so that it was completely in phase with the stationary bleached pattern, we get high fluorescence (F_{180}), and when we moved the monitoring beam completely out of phase with the bleached pattern we obtained a low fluorescence (F_0). We used the piezo-electric controller to oscillate the monitoring beam fringes.

To calculate A, the amplitude of the fringe pattern, an iterative process was used, based on the following algorithm:

1. We assumed a value for A.

2. Then, by integrating equation [22] for F_0 and F_{180} as functions of k, we generated a plot of $F_0 / \bar{F}$ and $(F_{180} - F_0)/\bar{F}$ versus k, using the Mathcad program. A typical resulting plot is shown in shown in Figure 6.

3. When the experimentally measured values of both $F_0 / \bar{F}$ and $(F_{180} - F_0)/\bar{F}$ at the same k value are correctly predicted by the graph, we conclude that the assumed A value is correct.

4. If not, we chose a different value of A and repeated the process.

From this exercise, the value of the amplitude was found to be unity. As a further check, different intensities of the photobleaching beam were used (that is different k values) to see if the A value chosen was satisfactory for all k. A was found to be equal to unity in all cases.
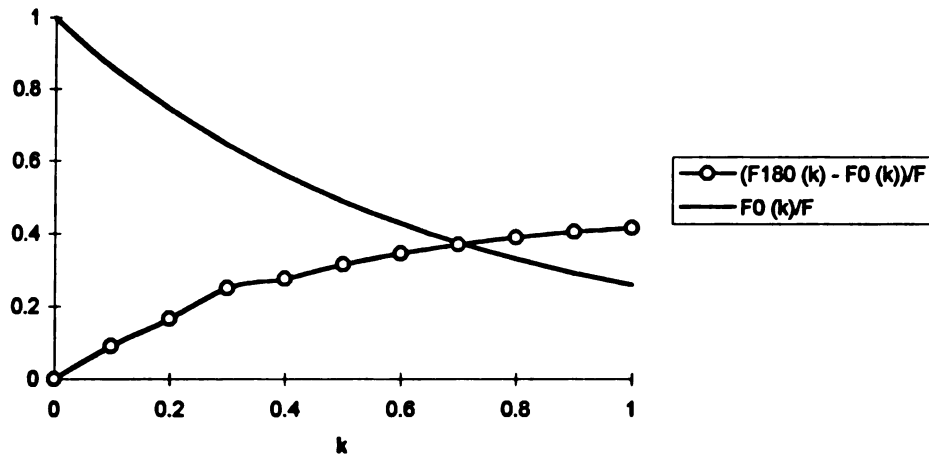
Figure 6. Graph used to calculate the amplitude of the fringe pattern.

4. RESULTS AND DISCUSSION

4.1 Check of the TIRF setup using steady state adsorption of BSA-FITC

The first exercise was to access the feasibility of using TIRF to characterize macromolecular interactions at the oil-water interface. To do this, we collected fluorescence intensity versus time data during the adsorption of BSA at the oil-water interface (Figure 7). Steady state adsorption was interpreted as a constant fluorescence intensity versus time. This initial experiment provides three important pieces of information:

1. It confirmed that the TIRF apparatus is functioning properly.

2. It helped establish the time required for adsorption to reach steady state after the pumping of the protein solution has been stopped. From the data, we estimated the time required for steady state to be approximately 15 minutes.

3. The profile in Figure 7 assures us that the intensity of the monitoring beam does not induce slow photobleaching of the adsorbed layer of protein molecules. If the monitoring beam intensity were high enough to cause photobleaching, a slow but steady decrease in the fluorescence signal would result. By adjusting the angles of the optical flats, we found that a monitoring beam intensity of ~15 μW is the optimum intensity to prevent slow photobleaching of the protein molecules, and yet produce fluorescence emissions that can be easily detected over the background noise level. For FRAPP experiments, the optimum monitoring beam intensity was 34 μW. The ratio of the monitoring beam to the photobleaching beam intensity was 1:5000.
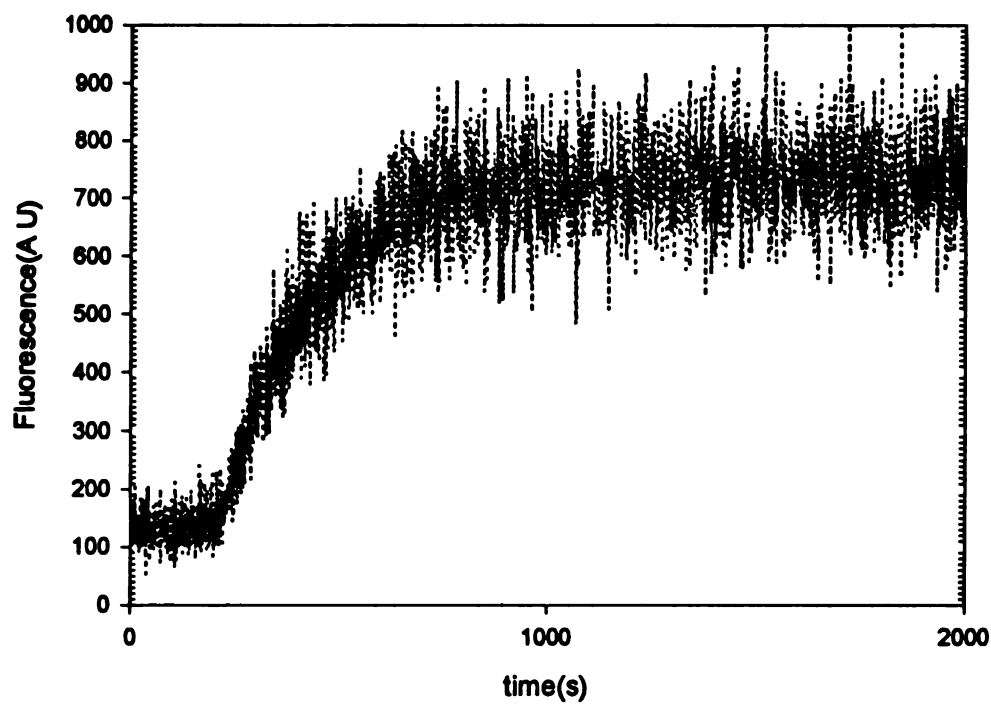
Figure 7. Fluorescence emission profile during adsorption of BSA at the oil-water interface. From this data, we estimated the time required for steady state adsorption to be 15 minutes.

After establishing that our setup was functioning proper of our setup, we ran an equilibrium adsorption experiment as explained in Section 3.3.4. We first introduced borax buffer into the cell. At time $t = 0$, we started injecting a labeled BSA solution into the cell. The fluorescence intensity rose steadily from a value of I_1, as shown in Figure 8, to a steady state value of I_3. We stopped the pumping and waited for a period of 10 minutes. We then replaced the labeled protein with an unlabeled protein solution of the same concentration. This resulted in a steady decrease in fluorescence emission until the signal reached a new steady state value of I_2.

The large difference in fluorescence intensity between I_3 and I_2 after the labeled protein solution in the bulk was replaced by unlabeled protein solution can be interpreted in one of two ways. It is possible that, contrary to what has been reported in the technical literature, protein adsorption at the oil-water interface is reversible, with the result that surface-adsorbed labeled proteins are immediately replaced by bulk unlabeled proteins, thus reducing the fluorescence emission intensity. The second possible explanation for this observation is that the majority of the fluorescence emission comes from the bulk solution, so that after the bulk was depleted of labeled proteins, there was a large drop in the fluorescence emission. To differentiate between these two possibilities, we will need to devise a calibration technique which can be used to calculate the concentration of proteins adsorbed at the interface solely in terms of the fluorescence emission intensity, and as a function of the concentration of the bulk solution. Such a calibration technique was described in chapter 3, although it was not implemented in this study due to time and equipment constraints at the time of this work.
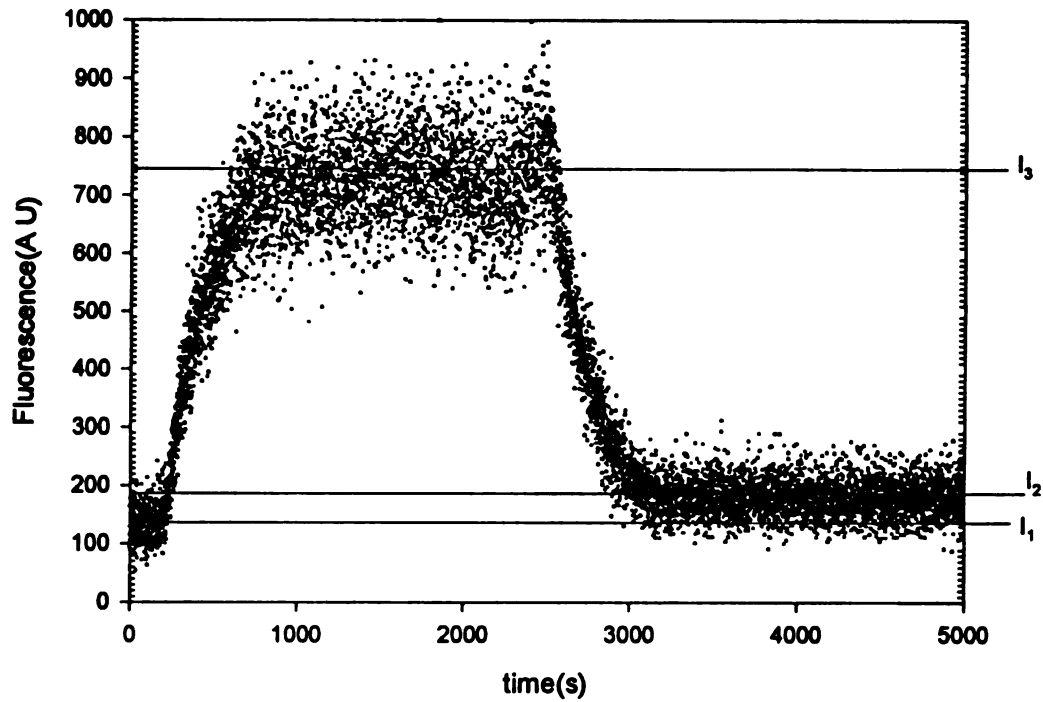
Figure 8. Fluorescence emission profile of BSA: at the initiation of the profile, unlabelled proteins in the sample cell were replaced by labeled proteins; after approximately 2500 seconds, the bulk labeled proteins were replaced by unlabeled proteins.

4.2 Results of spot photobleaching experiments

A typical profile of fluorescence recovery after photobleaching is shown in Figure 9. The original data, represented by the filled circles, were noisy over the entire range of recovery. To get a sense of the trend in the data, we averaged each set of eight consecutive data points sequentially (1-8, then 2-9, then 3-10, etc.) to obtain the points represented by the open squares. This process was done to make it easier to locate the prebleach and postbleach values with greater accuracy, since these are required in subsequent calculations. It must be pointed out that the regression line shown in Figure 9 is the same for both sets of data; the sequential averaging was done only to improve clarity.

The characteristic time, τ, was obtained by non-linear regression of the fluorescence recovery data using equation [30]. A typical regression analysis result is plotted in Figure 10 for the data shown in Figure 9. Results for the other two replicate experiments are shown in Figure 11 and Figure 12. The mobile fractions were calculated directly from equation [32]. The results of the three experiments are summarized in Table 1.

The average diffusion coefficient from the three experiments is $5.2 \pm 1 \times 10^{-8} \text{cm}^2/$ s, which is of the same order of magnitude (i.e., $\sim 10^{-8} \text{cm}^2/\text{s}$) as the value reported by Zimmermann et. al (1990). The average mobile fraction was $f = 0.77 \pm 0.05$.

Table 1. Diffusion coefficients and mobile fractions obtained from three replicate spot photobleaching experiments.

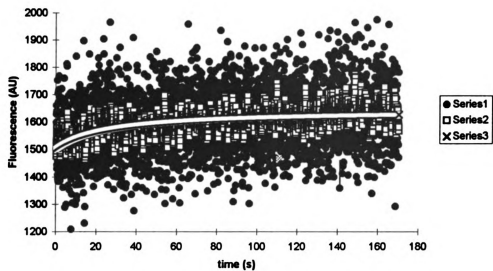| k	w (μm)	τ (sec)	D (cm^2/s) x 10^8	f
0.176	31.25	56.7 ± 0.7	4.3	0.79
0.282	31.25	50.1 ± 0.1	4.9	0.71
0.323	31.25	39.1 ± 0.2	6.2	0.81

Figure 9. Actual (Series 1), averaged (Series 2) and fitted (Series 3) fluorescence emission versus time after photobleaching.
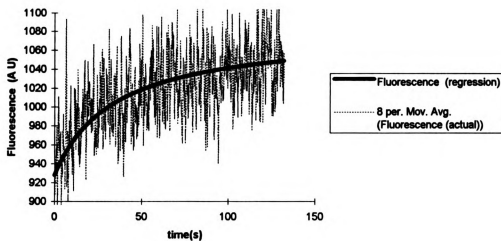

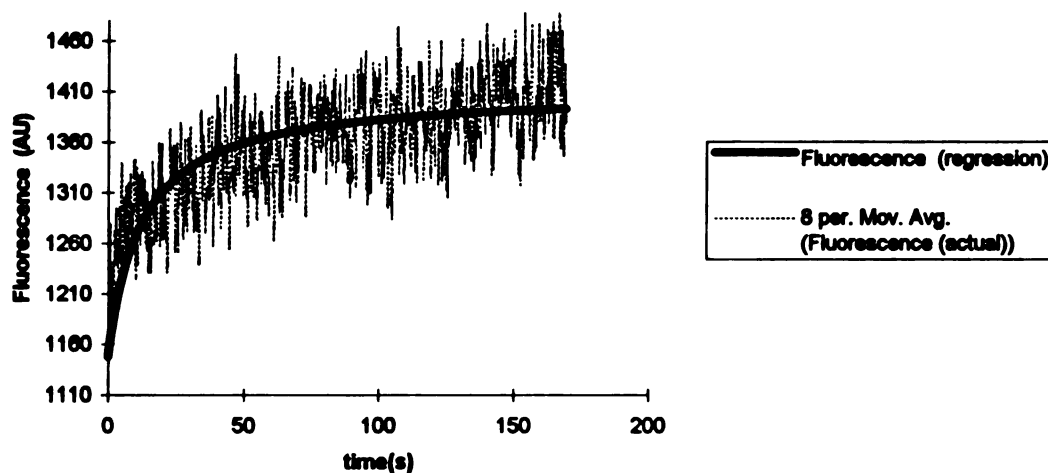Figure 10. Fluorescence recovery after photobleaching for a spot size of 31.25 μm

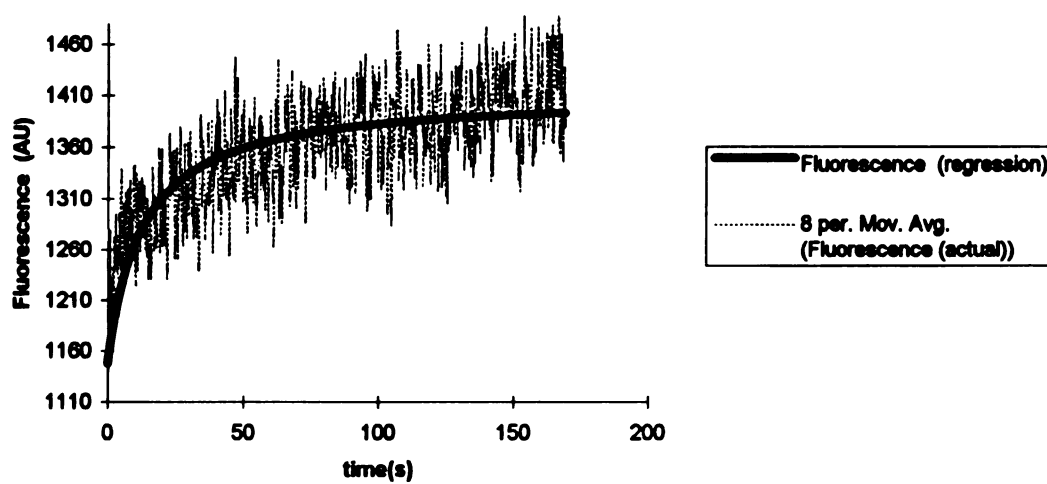Figure 11. Fluorescence recovery after photobleaching for a spot size of 31.25 μm

Figure 12. Fluorescence recovery after photobleaching for a spot size of 31.25 μm.

An average mobile fraction of ~0.4 has generally been reported in the technical literature for BSA adsorption at the glass-water interface (Robeson 1995, Tilton *et al.* 1990). A low mobile fraction indicates a high degree of irreversibility in protein adsorption. A high mobile fraction could also indicate that most of the recovery is due to exchange of the bleached near surface protein molecules with proteins from outside the field of the evanescent wave. We attempted to study this process further by coating the top slide with PEO and observing protein diffusion near this non-adsorbing interface to obtain an estimate for the near surface bulk diffusion. However, experimental results were inconclusive. So, at this stage, we are unable to distinguish between near surface diffusion and diffusion to the interface from the bulk. This is why we refer to the bulk diffusion coefficient as an apparent diffusion coefficient, since is most likely a combination of bulk and some surface diffusion.

4.3 Results of pattern photobleaching experiments

The results of three replicate FRAPP experiments are plotted in Figure 13, Figure 14, and Figure 15. In these figures, we have plotted the normalized rather than actual fluorescence data. The original fluorescence emission data were converted to normalized fluorescence emissions by the equation

$$Normalized\ Fluorescence = \frac{F(t) - \bar{F}}{F_0 - \bar{F}} \qquad [35]$$

where $F(t)$ is the fluorescence emission at any time, $\bar{F}$ is the post-bleach emission intensity, and F_o is the prebleach intensity.

The characteristic time for diffusion, τ, and the mobile fraction, f, were obtained by non-linear regression of the normalized fluorescence recovery data, using equation [33]. Equation [34] was used to further check the value of f obtained from the non-linear regression. It was found that the two methods gave the same result. The results are summarized in Table 2.
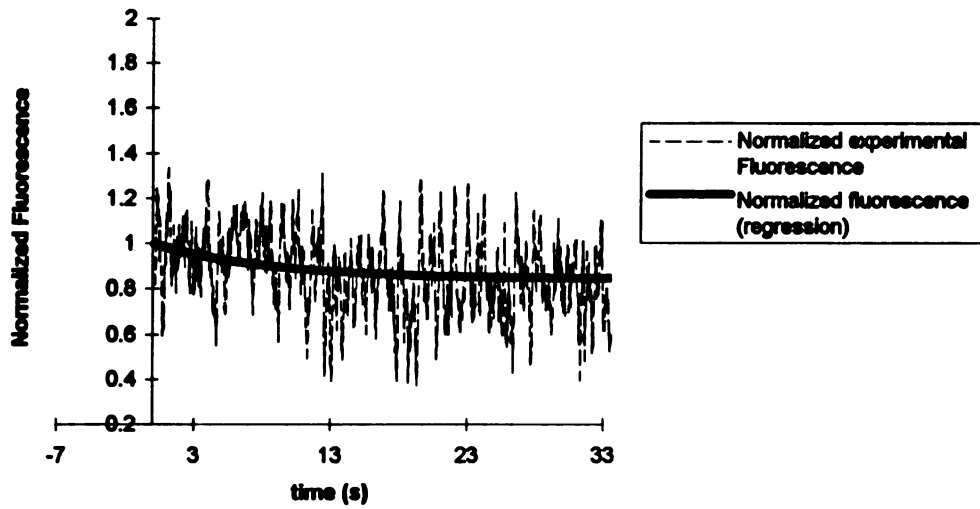
Figure 13. Normalized fluorescence recovery after pattern photobleaching with a fringe width of 6.25 μm.
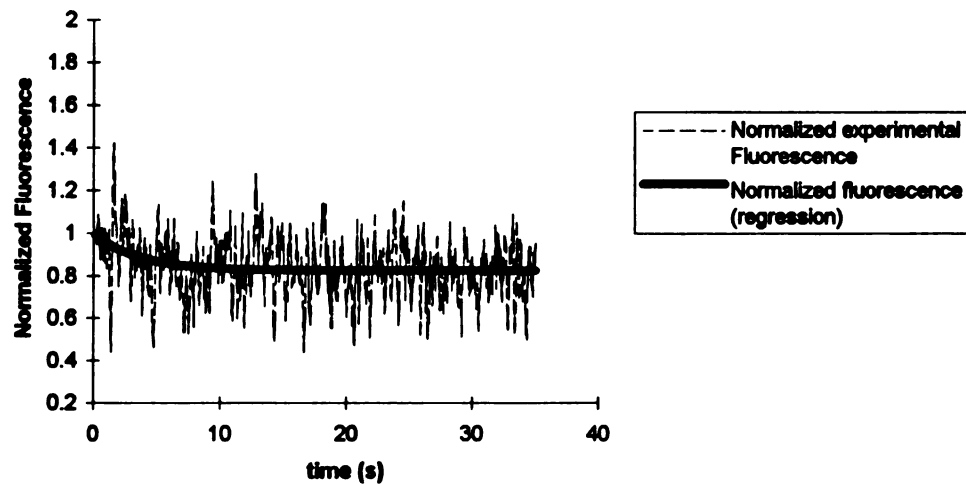
Figure 14. Normalized fluorescence recovery after pattern photobleaching with a fringe width of 5.68 μm.
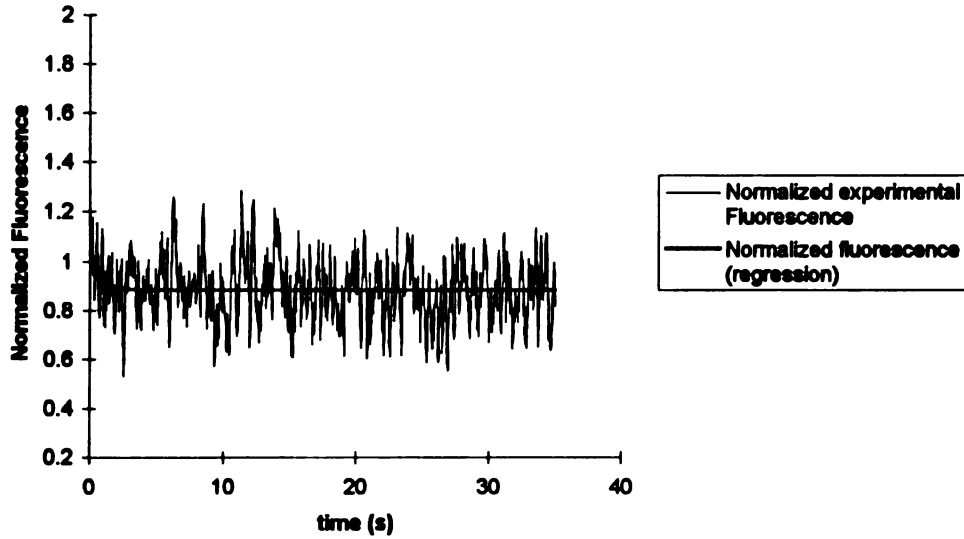
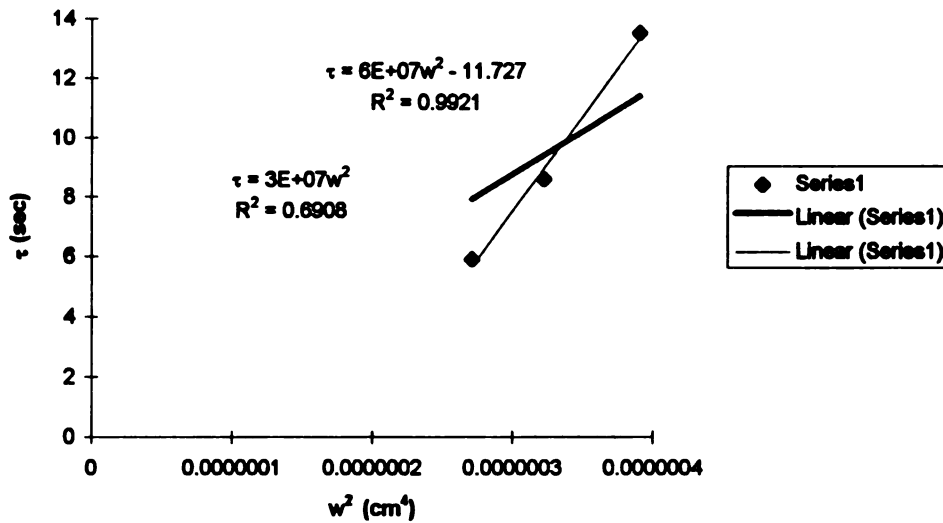Figure 15. Normalized fluorescence recovery after pattern photobleaching with a fringe width of 5.21 μm

Figure 16. Characteristic time of recovery versus the square of the fringe half period The thick line is for regression of the data through the origin, as required on physical grounds; the thin line is a best fit regression of the data.

Table 2. Characteristic times and mobile fractions from pattern photobleaching experiments

w (μm)	τ (sec)	f
6.25	13.5	0.48
5.68	8.6	0.53
5.21	5.9	0.45

A plot of τ "the characteristic time," vs. w^2 "the square of the characteristic length," is a straight line (Figure 16), which implies that the fluorescence recovery is purely by diffusion. If the fluorescence recovery were by flow, then the characteristic time would be proportional to w instead of w^2. Since all the experiments were run in a stopped flow format, this result is to be expected. The best fit regression of the data gave a regression coefficient of 0.99, but does not pass through the origin. However, on physical grounds, the plot of τ versus w^2 should pass through the origin. Forcing the regression line through the origin gives a low regression coefficient of 0.7, but satisfies the physics of the situation.

The slope of this plot gives a diffusion coefficient of $D = 3.38 \times 10^{-9}$ cm²/s, and an average mobile fraction of $f = 0.48 \pm 0.05$, both of which are slightly higher than the value reported by Tilton et. al (1990) ($D = 1.1 \times 10^{-9}$ cm²/s and $f = 0.42$) for EITC-BSA (Eosin isothiocyanate labeled BSA) adsorbing from a solution of 50μg/ml to the glass-water interface. Since EITC is a structural derivative of FITC, we do not expect it to affect the adsorption any differently than FITC, and certainly not to the extent of accounting for the observed differences. Therefore, it is necessary to look elsewhere for explanations.

The surface diffusion coefficient is a function of the surface concentration. Since we use a higher concentration of BSA than Tilton et. al (1990), we expect a lower diffusion coefficient for our experiment, since the interface is more "crowded." However, the

diff

the

diff

acc

In

tran

1.

2.

3.

4.

In

cm

is a

dep

ms

app

Pro

nea

flas

bei

wa

diffusion coefficient is also affected by hydrophobic interactions between the protein and the interface which, at this point, we do not fully understand. We suspect that the difference in hydrophobicities between our interface and that of Tilton et al. (1990) may account for the difference. However, this is currently under further study.

4.4 Discussion

In general, fluorescence recovery after photobleaching is possible due to four modes of transport:

1. exchange of unbleached bulk molecules with bleached molecules in the evanescent wave;

2. essentially one dimensional bulk diffusion-controlled exchange of bleached molecules with unbleached molecules near the interface, yet outside the field of the photobleaching pulse;

3. exchange of surface bleached molecules with unbleached molecules in the bulk; and

4. lateral diffusion of surface bound molecules.

In general, protein molecules are mobile in the bulk with a diffusion coefficient of $\sim 10^{-8}$ cm^2/s (Zimmermann et al. 1990). Therefore, the time for recovery from the first process is approximately given by equation [5]. In this study, l, the characteristic length is the depth of the evanescent wave (i.e. $l = 138$ nm), which implies a diffusion time of about 20 ms. As the time scale of our experiments is longer than 20ms, process 1 appears as an apparently unbleachable fraction in our experiments.

Process 2 is roughly of the same duration as the bleaching pulse. Consider a small area near the interface. The bleaching beam photobleaches this region during the time 't' it is flashed on the interface. The protein molecules in this region are however constantly being replaced by unbleached molecules from outside the field of view of the evanescent wave by approximately one dimensional diffusion. The region bleached by the beam is

about $(Dt)^{1/2}$. Depending on the time of photobleaching, it will take the unbleached molecules about the same time to replace the bleached molecules near the interface.

By using a bleaching beam diameter three times larger than the monitoring beam diameter, we can eliminate lateral diffusion as a probable cause of recovery because the approximate time of this diffusion, as calculated from equation [5] is on the order of 900 sec. Hence, the characteristic time measured by spot photobleaching is due to replacement of the surface bleached molecules by bulk molecules, and the replacement of near surface bleached protein molecules with molecules not in the field of view of the evanescent wave.

In pattern photobleaching, the bulk is free of labeled proteins, so the only recovery we obtain is due to lateral diffusion of labeled BSA along the interface. The value of the diffusion coefficient in spot photobleaching is an order of magnitude larger than the one obtained in pattern photobleaching, which tells us that we are indeed observing bulk diffusion in the spot photobleaching experiments.

In principle, rotational diffusion of BSA as it unfolds at the interface could also cause fluorescence recovery. However, since we have no indication that this effect plays a significant role in the time scale of our experiments, we did not attempt to quantify it here.

4.5 Possible sources of errors

The calculation of diffusion coefficients using the equation described by the model assumes that we can accurately locate the pre-bleach fluorescence intensity, the fluorescence intensity immediately after photobleaching, and the asymptote of the fluorescence recovery curve. The characteristic diffusion time, τ, is calculated based on a theoretical fit to the data, using the prebleach and post bleach beam intensities as end points. Due to the high noise level of our data over the whole range of recovery, we were not always able to obtain these points precisely.

In pattern photobleaching, the observable recovery is very small, as compared to spot photobleaching. So the error in determining the exact location of the prebleach and post bleach beam intensities is much higher. This error explains why the plot of the characteristic time versus the square of diffusion length in pattern photobleaching does not pass through origin. We suggest using a more sensitive photomultiplier tube, and reducing the gain and the high voltage settings of the PMT in future experiments.

The diffusion coefficient is proportional to the square of the beam size. As a result, discrepancy in measuring the spot size could create large errors in the diffusion coefficient. We assumed a perfectly Gaussian laser beam profile to calculate the beam width. However, imperfect optics and imperfect focusing of the beam can cause this assumption to break down as these effects make our beam profile non-Gaussian (Schneider and Webb 1981). Also, the mobile fraction measured in all spot photobleaching experiments was essentially the same. Since the mobile fraction does not depend on the beam size, we conclude that any errors in the calculation of the diffusion coefficient are due to errors in measuring the beam width. To overcome this problem, we suggest that the more elaborate procedure described by Schneider and Webb (1981) be used in subsequent studies.

5. SUMMARY AND CONCLUSIONS

The work done in this thesis has shown conclusively that total internal reflection fluorescence can be used to study macromolecular phenomena at the liquid-liquid interface and that our setup is functional. We have incorporated the capability to use both spot photobleaching (FPR) and pattern photobleaching (FRAPP) to determine both the bulk and lateral diffusion coefficients at the oil-water interface. We have estimated the time for steady state protein adsorption at the oil-water interface to be approximately 15 minutes from the initiation of the flow of proteins into the sample cell, based on a sample cell of approximately 1000μm in depth. The optimum monitoring beam intensity was found to be 15 μW, making the ratio of the monitoring to photobleaching beam intensity about 1:5000. The time required for photobleaching varied from 200 to 800 ms.

From the experiments conducted using TIRF/FRAPP, we have estimated that FITC-BSA has a lateral diffusion coefficient of 3.4×10^{-9} cm^2/s at the oil-water interface, with an average mobile fraction of 0.48. The apparent bulk diffusion coefficient obtained from TIRF/FPR experiments was 5.1×10^{-8} cm^2/s, with a mobile fraction of 0.77. The difference of one order of magnitude in the two results appears to indicate that the bulk diffusion of FITC-BSA is faster than lateral diffusion, as would be expected. We were unable to distinguish between diffusion of proteins in the bulk and the exchange of protein molecules between the bulk and the interface. This is because of the overlapping time scales of the two diffusion processes. Methods to differentiate between the two modes of recovery are currently under further study.

Errors in measuring the spot size, as well as signal noise strongly affected the values of the diffusion coefficients. We have analyzed how these errors might effect our readings and

might be used in future studies to calculate the surface concentration of proteins on the basis of fluorescence emission data. We have been unable to implement and verify the protocol in this study, because we have not yet developed a method for measuring surface concentrations independent of TIRF emissions.

6. SUGGESTIONS FOR FUTURE WORK

This thesis is an attempt to quantify protein adsorption at the liquid-liquid interface. We hope to provide a first approximation to far more complex studies dealing with ligand-receptor interactions, drug delivery and food processing problems. BSA was chosen because its characteristics are well documented in the literature. Also, various diffusion coefficients are reported for BSA adsorption at the solid-liquid interface which give an approximate idea of the value that should be obtained from our experiments. After reduction in the noise level of the signal and the protocol for estimating the accurate beam size has been established, we suggest the following experiments be conducted in the future.

6.1 Diffusion of surface-bound species

A beam expander should be used to increase the incident beam size, to enable a wider range of beam widths to work with. The beam can then be passed through pinholes of varying radii to change the spot size. Since the depth of the evanescent wave would remain constant in these experiments, the slope of the characteristic diffusion time versus the square of diffusion length will give the surface diffusion coefficient.

6.2 Diffusion of bulk species

We could obtain D_{bulk} by varying the depth of the evanescent wave while keeping the spot size constant. This is a very elegant technique because one could plot the recovery time versus the square of the characteristic length (d in this case) and obtain the bulk diffusion

run because, to change the depth of penetration of the evanescent wave, we need to either vary the wavelength or the incident angle of the laser beam. Changing the wavelength requires a tunable laser. We would also need fluorescence tags that will fluoresce at different wavelengths and different filters for our photomultiplier tube. Even if this was possible, various fluorescent tags will affect the diffusion characteristics of BSA in different ways. Also, varying angles of incidence will cause different spot sizes to form at the oil-water interface, making it impossible to maintain a given spot size while simultaneously varying the depth of penetration of the evanescent wave (Axelrod 1990).

Instead of the above procedure, it might be possible to vary the depth of the protein layer in the sample cell. This will change the depth of view of our evanescent wave while maintaining the spot size. We suggest three ways to do this:

1. The thickness of the PEO coating on the bottom slide could be varied. The thickness of the slide can then be measured by reflectometry to obtain the effective depth of the experimental cell.

2. We could use aluminum spacers of varying thickness (this will require O-rings of varying thickness) but constant area. Then, by measuring the thickness of the spacer, we could calculate the depth of view of the evanescent wave.

3. We could also insert quartz wafers of varying thickness into the sample cell to change the depth of the cell.

With each of the above modifications, the slope of a plot of recovery time with characteristic length will give D_{bulk}.

6.3 Accounting for concentration quenching

We are aware that, due to concentration quenching, the relative quantum yield of fluorophores may not be equal to unity as we have assumed in our analysis. Concentration quenching is a manifestation of Forster non-radiative energy transfer. In standard FPR and FRAPP analysis, we assumed the quantum yield of the fluorophores to be constant. We

know that, for our system, concentration quenching could occur at high labeling ratios as shown by Robeson (1995) for FITC-Rnase adsorbing to glass slides coated with polymer substrates. For this reason, labeling ratios were kept sufficiently lower than the concentration at which quenching of the signal might occur.

To account for a varying quantum yield, $q(r)$ must be brought inside the integral sign of equation [22]. Then, if fluorescence can be related to the surface concentration, a functional relationship between the relative quantum yield and the surface concentration can be obtained as explained by Robeson (1995). For this purpose, it is necessary to devise a calibration technique that can differentiate between bulk and interfacial fluorescence emissions, even at high labeling. This could be done by treating K, the instrument constant, as a variable. We could then try fitting experimental data to equation [10] to obtain K as a function of the concentration.

7. BIBLIOGRAPHY

1. Abney, J.R., Scalettar, B.A., and Thompson N.L. Evanescent interference patterns for fluorescence microscopy. *Biophys. J.* **61**:542-552 (1992).

2. Arai, K., Kusu, F., Takamura, K. Electrochemical behavior of drugs at the oil/water interfaces. In: *Liquid-Liquid Interfaces: Theory and Methods* 375-400 (1996).

3. Axelrod, D., Koppel, D.E., Schlessinger, J., Elson, E., Webb, W.W. Mobility measurements by analysis of fluorescence photobleaching recovery kinetics. *Biophysical Journal* **16**: 1055-1069 (1976).

4. Axelrod, D. Cell-substrate contacts illuminated by total internal reflection fluorescence. *J. Cell Biology* **89**: 141-145 (1981).

5. Axelrod, D., Thompson N.L and Burghart, T.P. Total internal reflection fluorescence microscopy. *J. Microscopy* **129** (pt 1) 19-28 (1983)

6. Axelrod, D., Burghart, T.P., and Thompson, N.L. Total internal reflection fluorescence. *Annu. Rev. Biophy. Bioeng.* **13**: 247-268 (1984).

7. Axelrod, D. Total internal reflection at biological surfaces. In: Noninvasive Techniques in Cell Biology, pages 93-127 (1990)

8. Axelrod, D. Hellen, E.H. and Fulbright R.M. In: Topics in Fluorescence Spectroscopy, Vol. 3 :Biomedical Applications. Lakowicz, J.R. (Editor), 289-243 (1992).

9. Barisas, G.B., and Leuther, M.D. Fluorescence photobleaching recovery measurement of protein absolute diffusion constants. *Biophysical Chemistry* **10**: 221-229 (1976).

10. Burghardt, T.P. and Axelrod D. Total internal reflection/fluorescence photobleaching recovery study of serum albumin adsorption dynamics. *Biophys. J.* **33**:455-468 (1981).

11. Cheng, Y.L., Darst, S. A., Robertson, C.R. Bovine Serum Albumin adsorption and desorption rates on solid surfaces with varying surface properties. *Journal of Colloid and Interface Sci.* **118**: 212-223 (1987).

12. Elson, E.L. Fluorescence correlation spectroscopy and photobleaching recovery.

13. Graham, D.E., Chatergoon, L. and Phillips, M.C. A technique for measuring interfacial concentrations at the oil-water interface. *Journal of Physics E. :Scientific Instruments* **8:** 696-699 (1975).

14. Hansen, R.L., Harris, J.L., Lateral diffusion of molecules partitioned into C-18 ligands on silica surfaces *Analytical Chemistry* **67:** 492-499 (1995).

15. Hirschfield, T. Total Reflection Fluorescence (TRF). *Can Spect.* 10:128.

16. Lakowicz, J.R., *Principles of Fluorescence Spectroscopy* :Plenum Press (1986)

17. Lok, B.K., Cheng, Y.-L., and Robertson, C.R. Total internal reflection fluorescence a technique for examining interactions of macromolecules with solid surfaces. *J. Colloid Interface Sci.* **91:** 87-103 (1983a)

18. Lok, B.K., Cheng, Y.-L., and Robertson, C.R. Protein adsorption on crosslinked polydimethyl siloxane using total internal reflection fluorescence. *J. Colloid Interface Sci.* **91:** 104-116 (1983b)

19. McKinney, R.M., Spillane, J.T., Pearce, G.W. A simple method for determining the labeling efficiency of fluorescein isothiocyanate products. *Analytical Biochemistry* **14:** 421-428 (1965)

20. Morrison, L.E. and Weber, G. Biological membrane modeling with a liquid-liquid interface. *Biophys. J.* **52:**367-379 (1987)

21. Nakanaga, T. and Takenaka, T. Resonance Raman spectra of monolayers of a surface-active dye adsorbed at the oil-water interface *J. Phys. Chem.* **81:** 645-649 (1977)

22. Robeson, J.L. *Application of TIRF to Probe Surface Diffusion and Orientation of Adsorbed Proteins*. Ph.D. Thesis, Carnegie Mellon University (1995)

23. Robeson, J.L. and Tilton, R.D. Effect of concentration quenching on fluorescence recovery after photobleaching measurements. *Biophysical J.* **68:** 2145-2155 (1995)

24. Schneider, M.B. Measurement of submicron laser beam radii. *Applied optics* 20:1382-1388 (Year).

25. Strauss, W.A. *Partial Differential Equations- an introduction* : John Wiley & Sons, Inc. (1992)

26. Takenaka, T. Effect of electrolyte on the molecular orientation in monolayers adsorbed at the liquid-liquid interface: studies by resonance Raman spectra. *Chem. Phys. Lett.* **55:**515-518 (1978)

27. Takenaka, T. and Nakanaga, T. Resonance Raman spectra of monolayers adsorbed at the interface between carbon tetrachloride and an aqueous solution of a surfactant and a dye. *J. Phys. Chem* **80**: 475-480 (1976).

28. Thomas, J., and Webb, W. W. Fluorescence photobleaching recovery: A probe of dembrane dynamics. In: *Noninvasive Techniques in Cell Biology,* 129-152 (1990)

29. Thompson, N.L. and Axelrod, D. Immunoglobin surface binding kinetics studied by total internal reflection with fluorescence correlation spectroscopy. *Biophys. J.* **43**: 103-114 (1983)

30. Thompson, N.L., Burghart, T.P. and Axelrod, D. Measuring surface dynamics of biomolecules by total internal reflection fluorescence with photobleaching recovery or correlation spectroscopy. *Biophys. J.* **33**: 435-454 (1981).

31. Tilton, R.D., Robertson, C.R., and Gast, A.P. Lateral diffusion of bovine serum albumin adsorbed at the solid-liquid interface. *J. Colloid Interface Sci.* **137**:192-203 (1990a).

32. Tilton, R.D., Robertson, C.R., and Gast, A.P. Surface diffusion of interacting proteins: effects of concentration on lateral mobility of adsorbed bovine serum albumin. *Biophys. J.* **58**: 1321-1326 (1990b).

33. Tweet, A.G., Gaines, G.L., and Bellamy, W.D. Fluorescence of chlorophyll * monolayers. *J. Chem. Phys.* 40:2596-2600 (1964).

34. Volkov, A.G., Deamer, D.W. Oil/water interfaces and the origin of life. In: *Liquid-Liquid interfaces: Theory and Methods* 363-375 (1996).

35. Zimmermann, R.M., Schmidt, C. F., and Gaub, H. E. Absolute quantities and equilibrium kinetics of macromolecular adsorption by fluorescence photobleaching in total internal reflection *Journal of Colloid and Interface Science* **139**: 1, 268-280 (1990).

8. APPENDIX: MATHCAD PROGRAM

Mathcad program used to develop the fluorescence profile for the immobilized fluorophore system
Method to calculate the amplitude of the fluorescence fringe pattern

Assume A

$A := 1$

$\pi := 3.141592654$

$k := 0, 0.02 .. 1$

unitless profile for the photobleaching beam and the monitoring beam when it is not in phase with the bleached pattern

$I(X) := 1 + A \cdot \sin(\pi X)$

unitless profile of the monitoring beam shifted by a phase

$I\pi(X) := 1 + A \cdot \sin(\pi X + \pi)$

Fluorescence observed from the immobilized fluorophore system when the monitoring beam has not been shifted so that it is alligned to the bleached region divided by fluorescence before photobleaching

$$F0(k) := \frac{\displaystyle\int_{-1}^{1} \exp(-k \cdot I(X)) \cdot I(X) \, dX}{2}$$

Fluorescence observed from the immobilized fluorophore system when the monitoring beam has been shifted so that it is alligned to the bleached region divided by fluorescence before photobleaching

$$F180(k) := \frac{\displaystyle\int_{-1}^{1} \exp(-k \cdot I(X)) \cdot I\pi(X) \, dX}{2}$$

$y(k) := F180(k) - F0(k)$